Artificial light-harvesting system based on ESIPT-AIE-FRET triple fluorescence mechanism

Tangxin Xiao[a,b,*], Cheng Bao[a], Liangliang Zhang[a], Kai Diao[a], Dongxing Ren[a], Chunxiang Wei[b,*], Zheng-Yi Li[a], Xiao-Qiang Sun[c]

[a]School of Petrochemical Engineering, Changzhou University, Changzhou 213164, China.

E-mail: xiaotangxin@cczu.edu.cn

[b]Department of Chemistry, University of Cambridge, Cambridge CB2 1EW, UK

E-mail: cw794@cam.ac.uk

[c]Institute of Urban & Rural Mining, Changzhou University, Changzhou 213164, China

Table of Contents

1. Supplementary characterization of L NPs

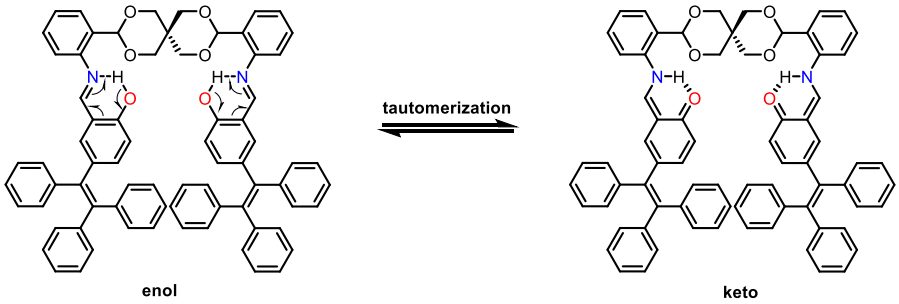

Scheme S1 The enol and keto forms of compound **L**.

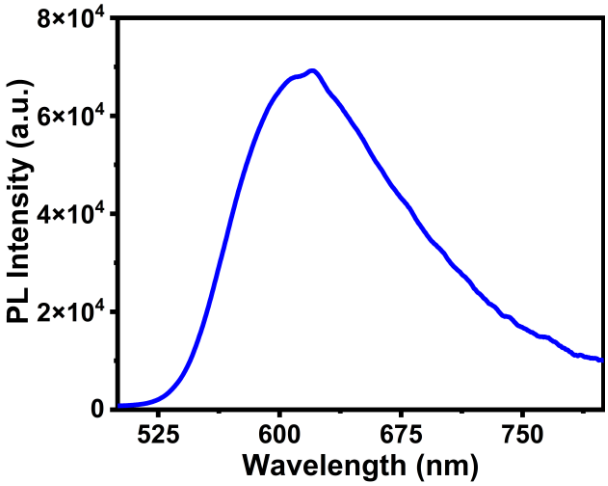

Fig. S1. Solid-state fluorescence spectrum of **L** (λ_{ex} = 327 nm).

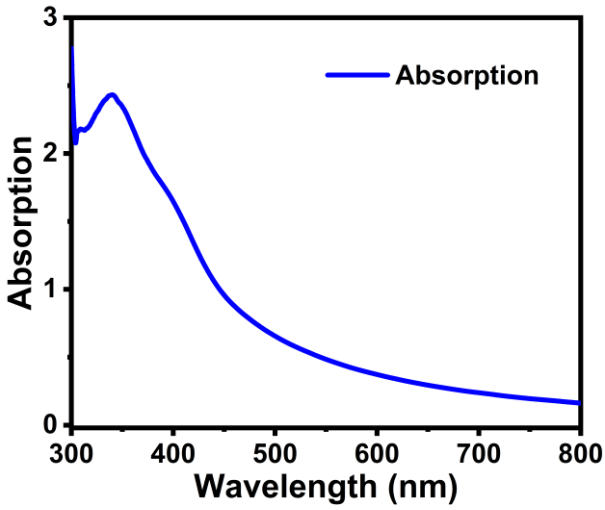

Fig. S2. UV-vis absorption spectrum of **L** nanoparticles (NPs) in mixed THF/H_2O (f_w = 90%). [**L**] = 2×10^{-5} M.

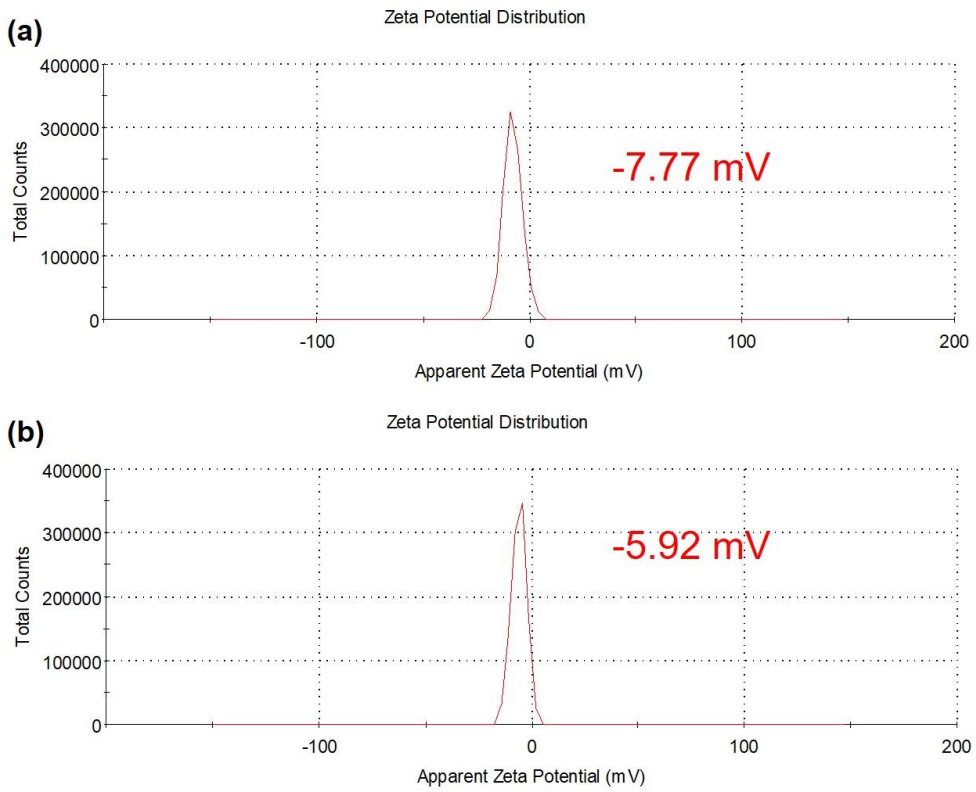

Fig. S3. Zeta-potentials of (a) **L** NPs, (b) **L-NDI** NPs. [**L**] = 2.00 × 10^{-5} M and [**NDI**] = 1 × 10^{-7} M, respectively.

2. Supplementary characterization of L-NDI LHS

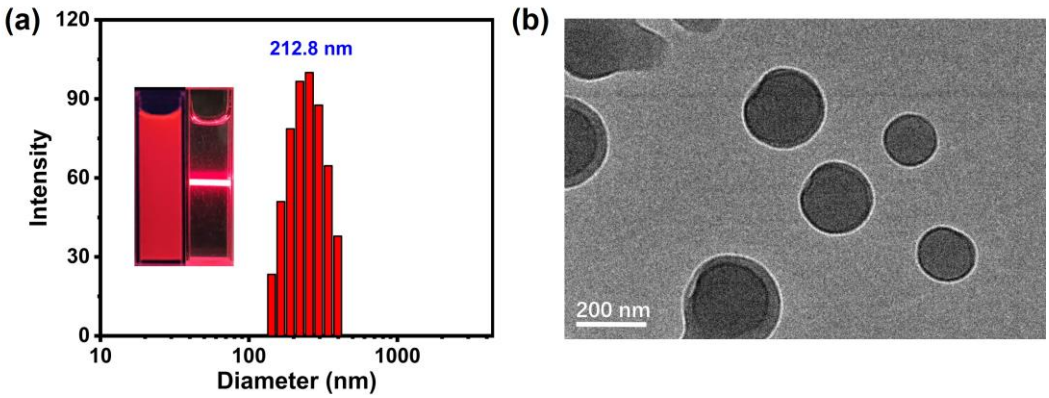

Fig. S4. (a) DLS data of **L-NDI** in THF/water (f_w = 90%). (b) TEM image of **L-NDI** NPs.

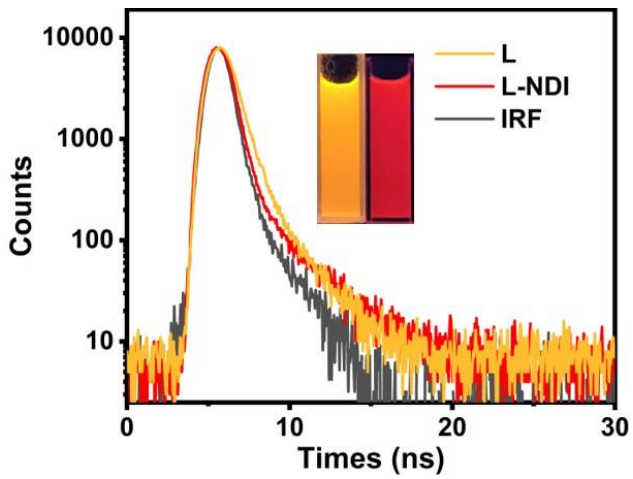

Fig. S5. Fluorescence decay profiles of **L** NPs (orange line) and **L-NDI** NPs (red line), inset: fluorescent photographs of **L** NPs (left) and **L-NDI** NPs (right).

Table S1 Fluorescence lifetimes of **L** and **L-NDI** (D:A = 200:1) upon excitation at 327 nm, [**L**] = 2.00×10^{-5} M, [**NDI**] = 1.00×10^{-7} M, respectively.

Sample	τ_1/ns	**RW1**[%]	τ_2/ns	**RW2**[%]	τ/ns	χ^2
L	0.50	25.54	2.69	74.46	2.13	1.092
L-NDI (**L** : **NDI** = 200 : 1)	0.64	66.86	2.04	33.14	1.10	1.109

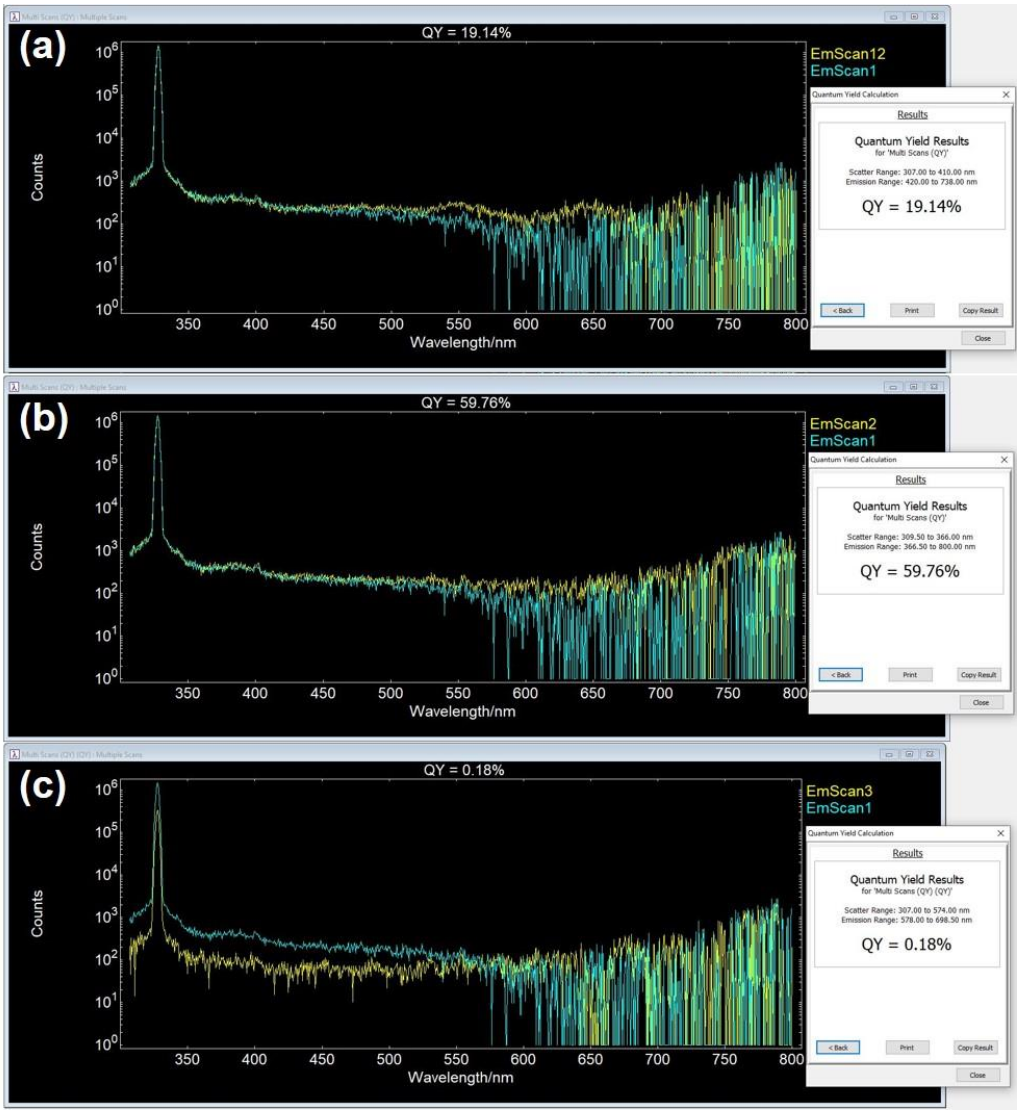

Fig. S6. Absolute fluorescence quantum yields ($\Phi_{f(abs)}$) (a) of **L**, (b) of **L-NDI** (**L**/**NDI** = 400/1), (c) of **L** + Cu^{2+} (**L**/Cu^{2+} = 1/1), upon excitation at 327 nm in aqueous solution. [**L**] = 2.00 × 10^{-5} M.

Table S2 Fluorescence quantum yields of **L** and **L-NDI**. [**L**] = 2.00 × 10^{-5} M, [**NDI**] = 1.00 × 10^{-7} M, respectively.

Sample	Flourescence quantum yields ($\Phi_{f(abs)}$)
L	19.14%
L-NDI (**L** : **NDI** = 200 : 1)	59.76%
L + Cu^{2+} (1:1)	0.18%

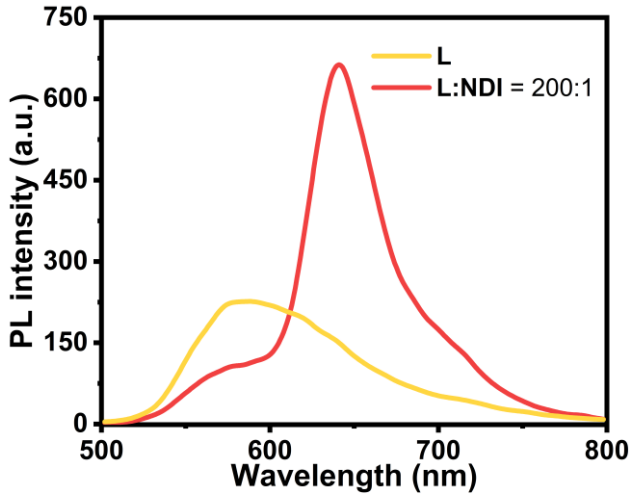

Fig. S7. Fluorescence spectra of **L** and **L-NDI** (D:A = 200:1) assembly upon excitation at 327 nm.

Energy-transfer efficiency (Φ_{ET}) was calculated from fluorescence spectra by the equation S1[S1]:

$$\mathbf{\Phi_{ET} = 1 - I_{DA} / I_D} \text{ (eq. S1)}$$

Where $\mathbf{I_{DA}}$ and $\mathbf{I_D}$ are the fluorescence intensities of **L-NDI** (donor and acceptor) and **L** (donor) at 585 nm when excited at 327 nm, respectively.

Table S3 Energy-transfer efficiency with different **L/NDI** ratio.

Sample	**Concentration, respectively**	**Energy-transfer efficiency (Φ_{ET})**
L-NDI (**L** : **NDI** = 200 : 1)	[**L**] = 2.00 × 10^{-5} M [**NDI**] = 1.00 × 10^{-7} M	50.2%
L-NDI (**L** : **NDI** = 300 : 1)	[**L**] = 2.00 × 10^{-5} M [**NDI**] = 6.67 × 10^{-8} M	41.1%
L-NDI (**L** : **NDI** = 400 : 1)	[**L**] = 2.00 × 10^{-5} M [**NDI**] = 5.00 × 10^{-8} M	36.9%
L-NDI (**L** : **NDI** = 500 : 1)	[**L**] = 2.00 × 10^{-5} M [**NDI**] = 4.00 × 10^{-8} M	32.8%
L-NDI (**L** : **NDI** = 750 : 1)	[**L**] = 2.00 × 10^{-5} M [**NDI**] = 2.67 × 10^{-8} M	25.2%
L-NDI (**L** : **NDI** = 1000 : 1)	[**L**] = 2.00 × 10^{-5} M [**NDI**] = 2.00 × 10^{-8} M	18.3%
L-NDI (**L** : **NDI** = 2000 : 1)	[**L**] = 2.00 × 10^{-5} M [**NDI**] = 1.00 × 10^{-8} M	9.6%

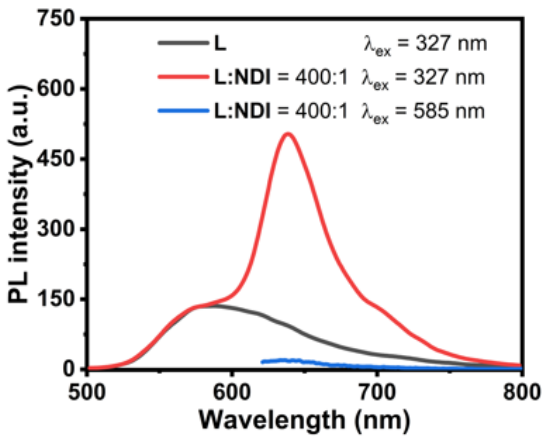

Fig. S8. Fluorescence spectra of **L-NDI** (red line: λ_{ex} = 327 nm; blue line: λ_{ex} = 585 nm). The black line represents the fluorescence spectrum of **L**, which was normalized according to the fluorescence intensity at 585 nm of the red line. [**L**] = 2.00 × 10^{-5} M, [**NDI**] = 5.00 × 10^{-8} M, respectively.

The antenna effect (AE) was calculated based on the emission spectra using equation S2[S1]:

$$\mathbf{AE = I'_{DA,327} / I_{DA,585} = (I_{DA,327} - I_{D,327}) / I_{DA,585}} \text{ (eq. S2)}$$

Where $\mathbf{I_{DA,327}}$ and $\mathbf{I_{DA,585}}$ are the fluorescence intensities at 640 nm with the excitation of the light-harvesting system at 327 nm and 585 nm, respectively. $\mathbf{I_{D,327}}$ is the fluorescence intensities at 640 nm of **L**, which was normalized with the **L-NDI** assembly at 585 nm.

Table S4 Antenna effect with different **L**/**NDI** ratio.

Sample	Concentration, respectively	AE
L-NDI (**L** : **NDI** = 200 : 1)	[**L**] = 2.00 × 10^{-5} M [**NDI**] = 1.00 × 10^{-7} M	20.9
L-NDI (**L** : **NDI** = 300 : 1)	[**L**] = 2.00 × 10^{-5} M [**NDI**] = 6.67 × 10^{-8} M	21.1
L-NDI (**L** : **NDI** = 400 : 1)	[**L**] = 2.00 × 10^{-5} M [**NDI**] = 5.00 × 10^{-8} M	23.0
L-NDI (**L** : **NDI** = 500 : 1)	[**L**] = 2.00 × 10^{-5} M [**NDI**] = 4.00 × 10^{-8} M	16.7
L-NDI (**L** : **NDI** = 750 : 1)	[**L**] = 2.00 × 10^{-5} M [**NDI**] = 2.67 × 10^{-8} M	15.4
L-NDI (**L** : **NDI** = 1000 : 1)	[**L**] = 2.00 × 10^{-5} M [**NDI**] = 2.00 × 10^{-8} M	13.4
L-NDI (**L** : **NDI** = 2000 : 1)	[**L**] = 2.00 × 10^{-5} M [**NDI**] = 1.00 × 10^{-8} M	6.6

3. Control experiment based on compound C

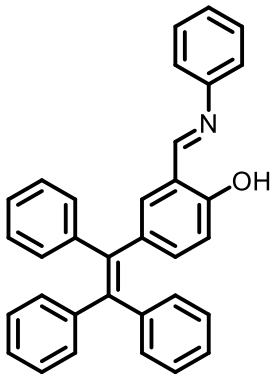

Scheme S2 Chemical structure of **C**.

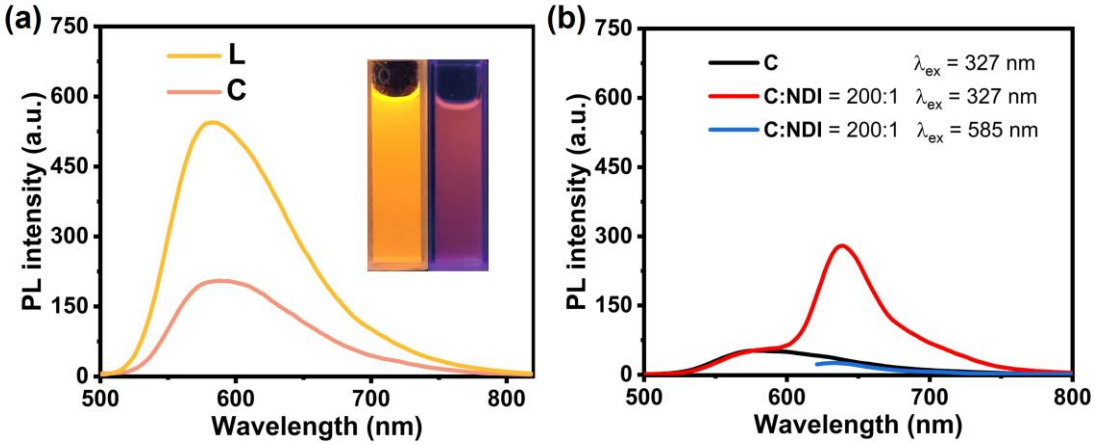

Fig. S9. (a) Fluorescence spectra of **L** and **C** NPs. [**L**] = 2.00 × 10^{-5} M, [**C**] = 4.00 × 10^{-5} M. λ_{ex} = 327 nm. (b) Fluorescence spectra of **C-NDI** (red line: λ_{ex} = 327 nm; blue line: λ_{ex} = 585 nm). The black line represents the fluorescence spectrum of **C**, which was normalized according to the fluorescence intensity at 585 nm of the red line. [**C**] = 2.00 × 10^{-5} M, [**NDI**] = 1.00 × 10^{-7} M, respectively.

Table S5 The antenna effect value of **C-NDI**

Sample	Concentration	AE
C-NDI (**C** : **NDI** = 200 : 1)	[**C**] = 2.00 × 10^{-5} M [**NDI**] = 1.00 × 10^{-7} M	8.4

4. Cu^{2+} sensing by L and L-NDI

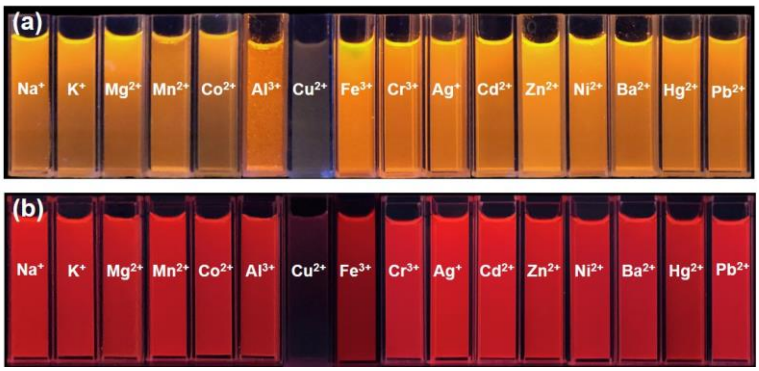

Fig. S10. Photograph (a) of compound **L** (b) of compound **L-NDI** interacting with metal ions under a 365 nm UV lamp.

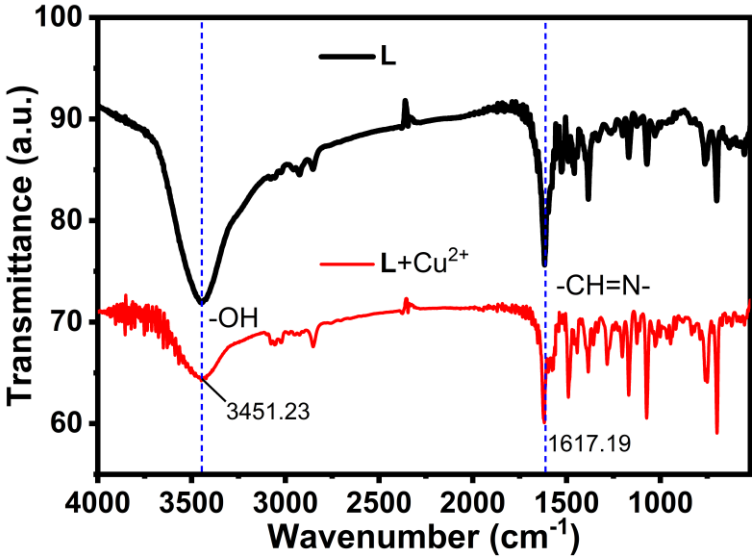

Fig. S11. FT-IR spectra of **L** and **L** + Cu^{2+}.

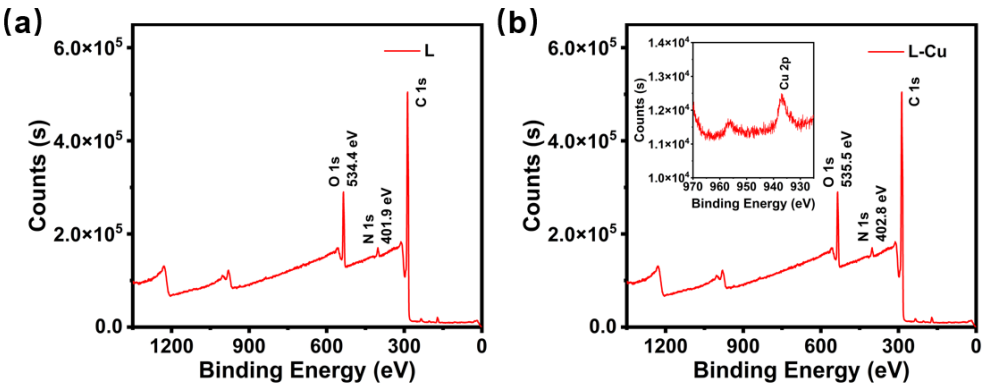

Fig. S12. XPS spectra of (a) **L** NPs and (b) **L**-Cu NPs, inset: enlarged picture of the Cu $2p_{3/2}$ binding energy.

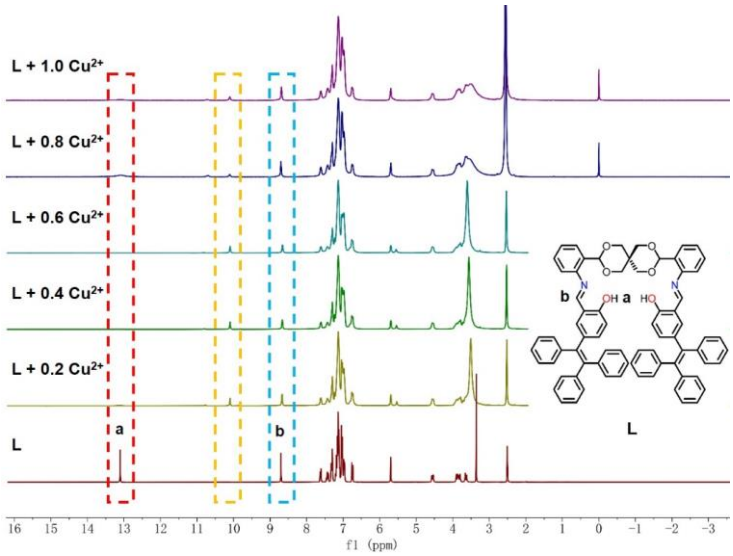

Fig. S13. ^{1}H NMR titration spectra of **L** on increasing concentrations of Cu^{2+} in DMSO-d_6 solution.

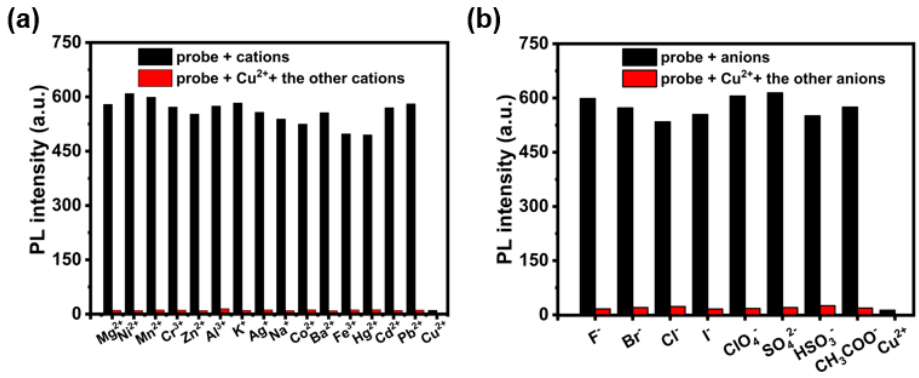

Fig. S14. Bar diagram of the competitive experiments of various metal cations (a) and anions (b) on the fluorescence intensity of the **L**-Cu^{2+} complex ($\lambda_{ex.}/\lambda_{em.}$ = 327/585 nm).

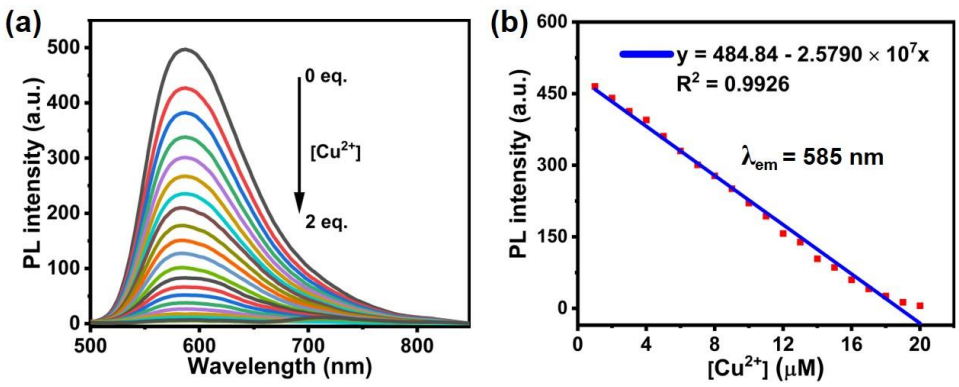

Fig. S15. (a) The fluorescent titration experiment of **L** (20 μM) to detect Cu^{2+} ($\lambda_{ex.}$ = 327 nm, $\lambda_{em.}$ = 585 nm). (b) The relationship between fluorescence intensity of the system at 585 nm and Cu^{2+} concentration (0 μM–20 μM).

5. Synthesis of compound L and C

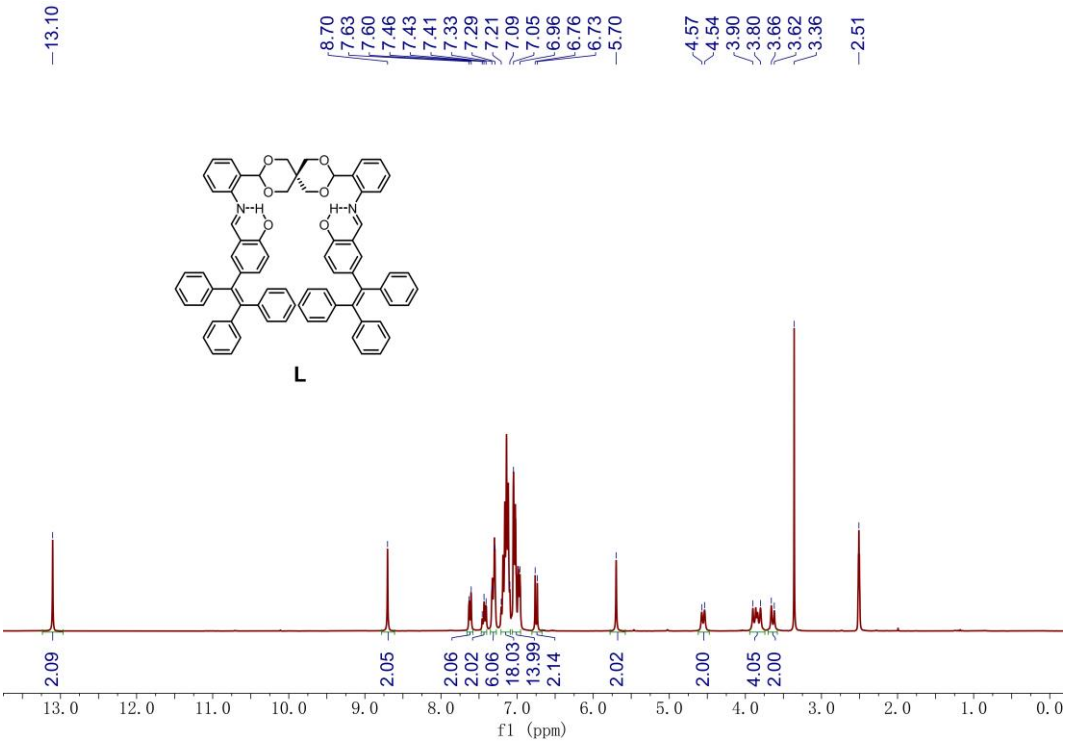

Fig. S16. ^{1}H NMR spectrum (300 MHz, DMSO-d_6, 298 K) of compound **L**.

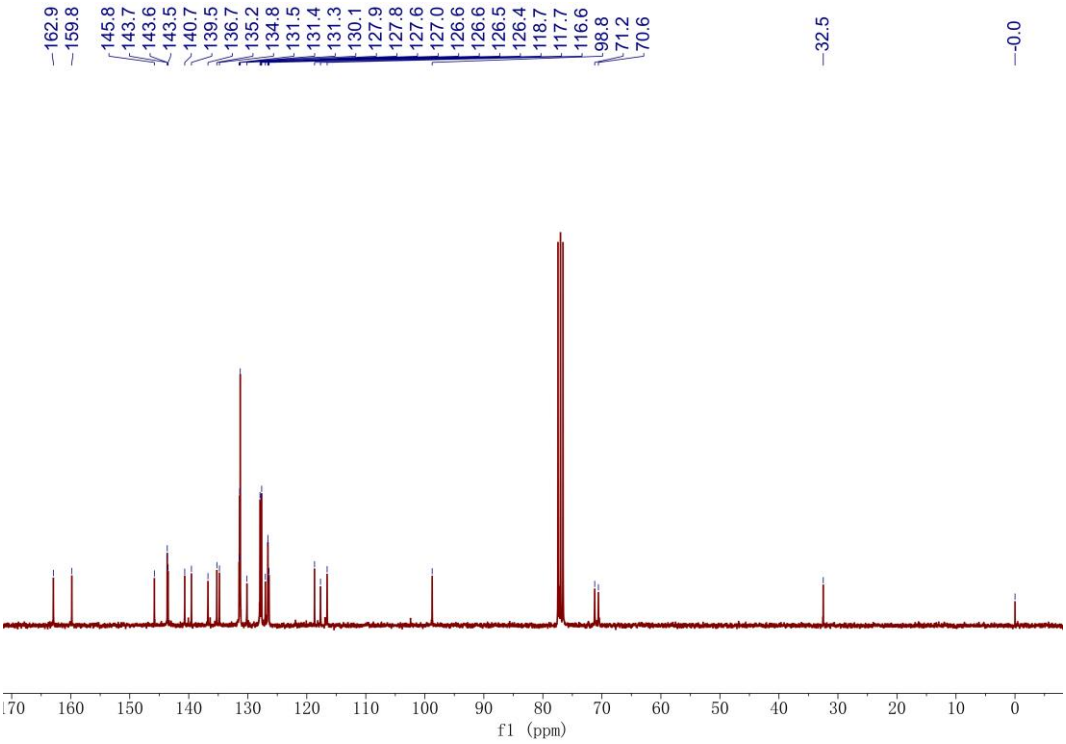

Fig. S17. ^{13}C NMR spectrum (75 MHz, $CDCl_3$, 298 K) of compound **L**.

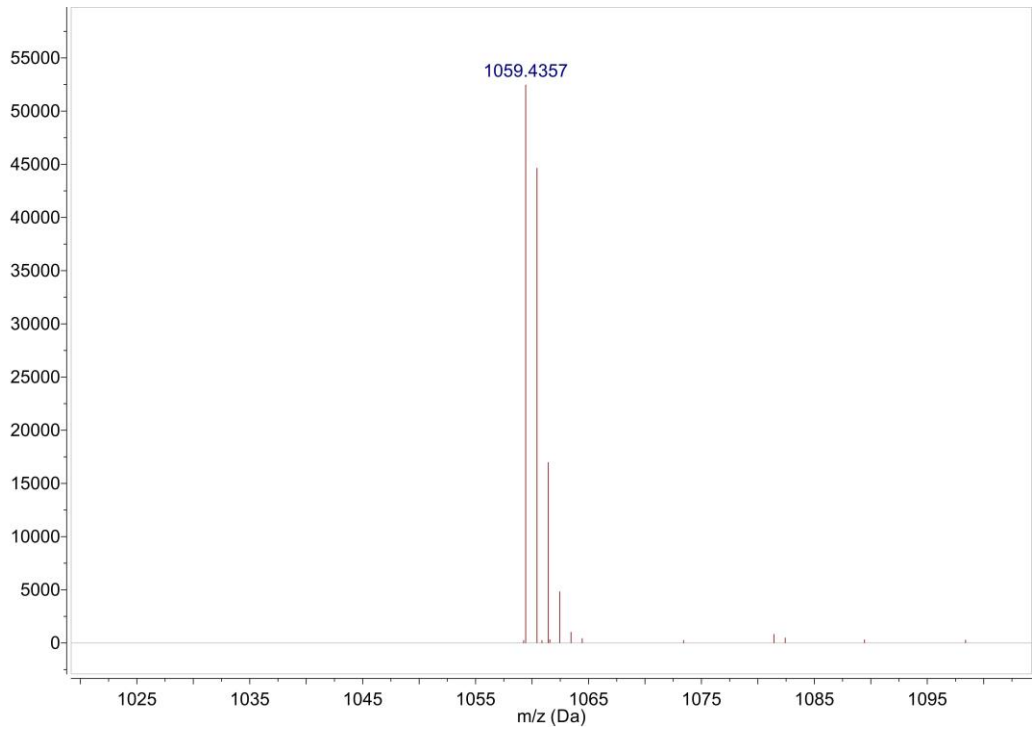

Fig. S18. HR-MS (ESI, positive mode, CH_3CN) of **L**.

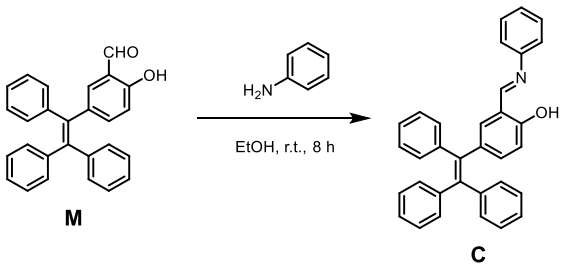

Scheme S2 Synthesis of **C**

Synthesis of **C**: a mixture of **M** (150.0 mg, 0.4 mmol) and aniline (40.0 μL, 0.4 mmol) in 10 mL anhydrous ethanol solution was stirred for 8 h at room temperature. The mixture was filtered and the precipitate was washed with ethanol for three times. The solid was dried under vacuum at 50 ºC to obtain the product as a fluffy powder (165.5 mg, yield 92%). ^{1}H NMR (300 MHz, DMSO-d_6): δ (ppm) = 13.10 (s, 1H, Ar-O*H*), 8.76 (s, 1H, N=C*H*), 7.45-7.26 (m, 6H, Ar-*H*), 7.20-7.10 (m, 9H, Ar-*H*), 7.04-6.95 (m, 7H, Ar-*H*), 6.72 (d, *J* = 8.4 Hz, 1H, Ar-*H*). ^{13}C NMR (75 MHz, DMSO-d_6): *δ* (ppm) = 163.5, 159.5, 148.3, 143.7, 143.5, 140.8, 140.1, 136.3, 134.9, 134.6, 131.2, 131.2, 131.1, 129.9, 128.4, 128.4, 128.3, 127.4, 127.1, 127.0, 127.0, 121.8, 119.3, 116.6. HR-ESI-MS: *m/z* calcd for $C_{33}H_{25}NO$ $[M + H]^+$= 452.2009, found = 452.2007.

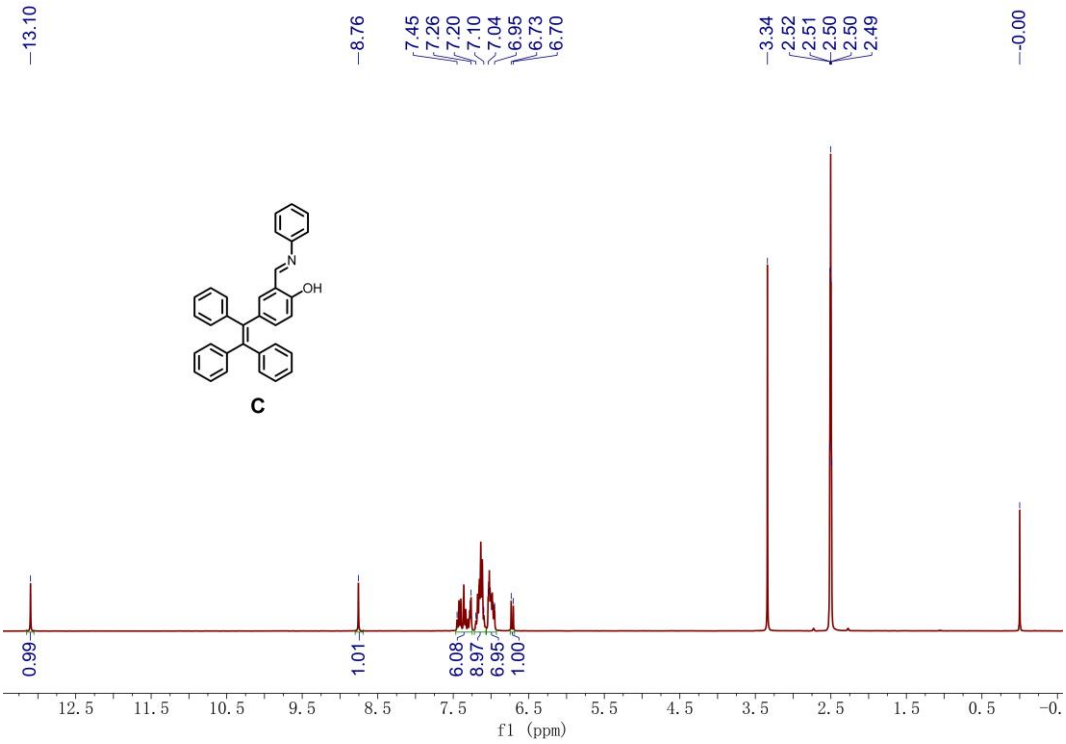

Fig. S19. ^{1}H NMR spectrum (300 MHz, DMSO-d_6, 298 K) of the control compound **C**.

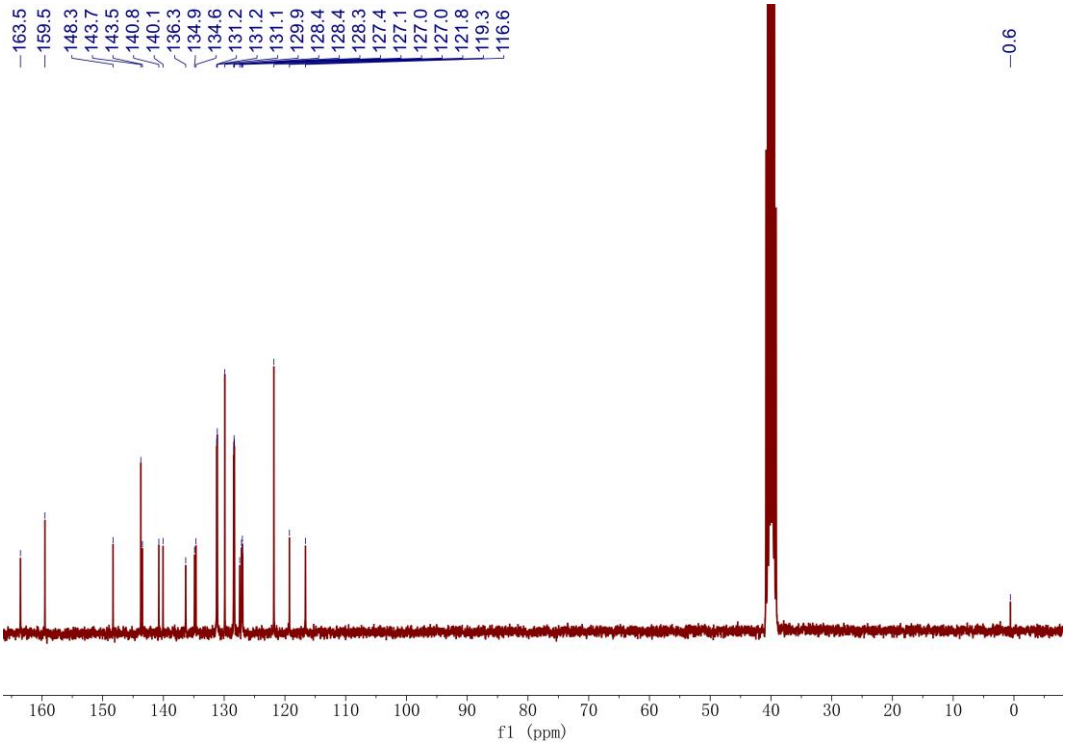

Fig. S20. ^{13}C NMR spectrum (75 MHz, DMSO-d_6, 298 K) of contrast compound **C**.

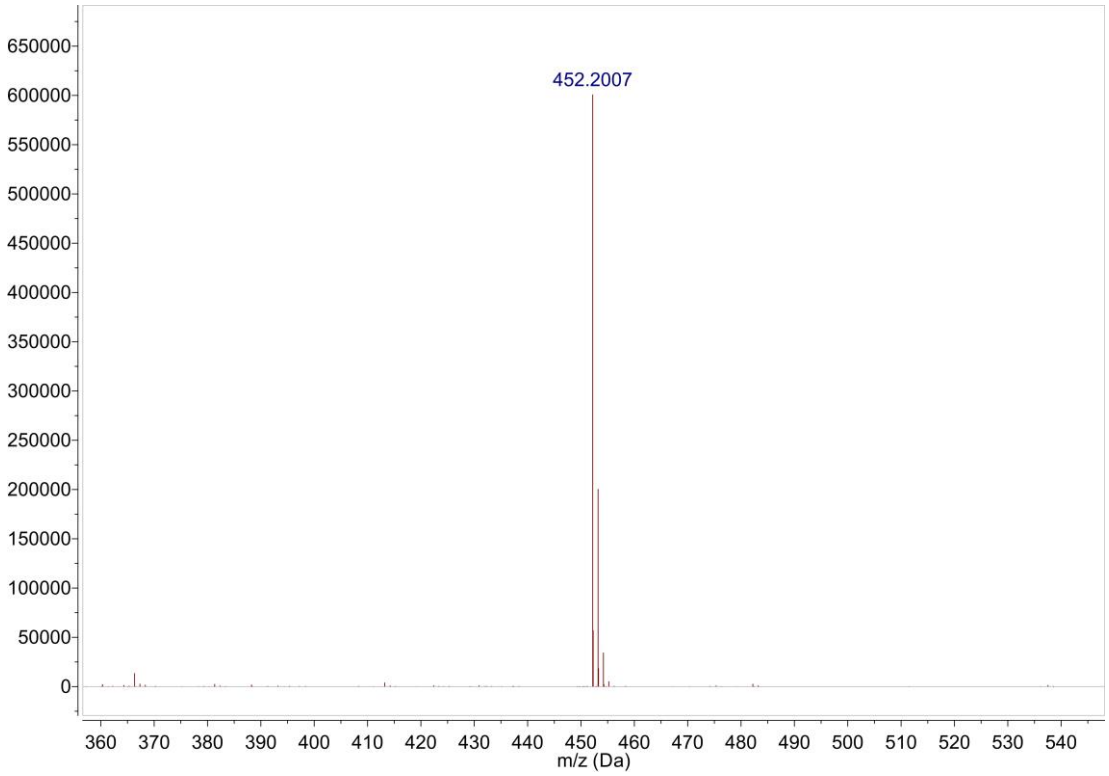

Fig. S21. HR-MS (ESI, positive mode, CH_3CN) of **C**.

6. References

[S1] Hao, M.; Sun, G.; Zuo, M.; Xu, Z.; Chen, Y.; Hu, X.-Y.; Wang, L. *Angew*. *Chem*. *Int*. *Ed*. **2020**, *59*, 10095-10100.

[S2] Zhao, Y.-H.; Luo, Y.; Wang, H.; Guo, T.; Zhou, H.; Tan, H.; Zhou, Z.; Long, Y.; Tang, Z. *ChemistrySelect* **2018**, *3*, 1521–1526.

[S3] Li, Z.-Y.; Su, H.-K.; Zhou, K.; Yang, B.-Z.; Xiao, T.; Sun, X.-Q.; Jiang, J.; Wang, L. *Dyes Pigments* **2018**, *149*, 921–926.